AAC Journals.ASM.org

Effectiveness of Antimicrobial Peptide Immobilization for Preventing Perioperative Cornea Implant-Associated Bacterial Infection

Xiao Wei Tan,[a] Tze Wei Goh,[a] P. Saraswathi,[b] Chan Lwin Nyein,[a] Melina Setiawan,[a] Andri Riau,[a] R. Lakshminarayanan,[b,e] Shouping Liu,[b,e] Donald Tan,[c,d,e] Roger W. Beuerman,[b,c,f] Jodhbir S. Mehta[a,b,d,e]

Tissue Engineering and Stem Cell Group, Singapore Eye Research Institute, Singapore[a]; Antimicrobials Group, Singapore Eye Research Institute, Singapore[b]; Yong Loo Lin School of Medicine, National University of Singapore, Singapore[c]; Singapore National Eye Centre, Singapore[d]; Duke-NUS Graduate Medical School, Singapore[e]; Duke-NUS SRP Neuroscience and Behavioral Disorders, Singapore[f]

Titanium (Ti) is a promising candidate biomaterial for an artificial corneal skirt. Antimicrobial peptide (AMP) immobilization may improve the bactericidal effect of the Ti substrate. In this study, we tested the bactericidal efficacy of a functionalized Ti surface in a rabbit keratitis model. A corneal stromal pocket was created by a femtosecond laser. The Ti films were then inserted into the pocket, and *Staphylococcus aureus* or *Pseudomonas aeruginosa* was inoculated into the pocket above the implant films. The corneas with Ti-AMP implants were compared with the corneas implanted with unprotected Ti by slit lamp observation and anterior segment optical coherence tomography (AS-OCT). Inflammatory responses were evaluated by bacterium counting, hematoxylin-eosin staining, and immunostaining. There was a lower incidence and a lesser extent of infection on rabbit corneas with Ti-AMP implants than on those with unprotected Ti implants. The bactericidal effect of AMP against *S. aureus* was comparable to that of postoperative prophylactic antibiotic treatment; hence, SESB2V AMP bound to the Ti implant provided functional activity *in vivo*, but its efficacy was greater against *S. aureus* than against *P. aeruginosa*. This work suggests that SESB2V AMP can be successfully functionalized in a rabbit keratitis model to prevent perioperative corneal infection.

Infection or biofilm formation on the surface of implants following the implantation of surgical devices is a clinically devastating complication that accounts for about 60% of all hospital-associated infections (1). Devices that penetrate the skin or those that are within tissues, e.g., the cornea, present the highest risks for infection (2, 3). Endophthalmitis, a severe panocular infection, remains one of the most devastating complications after the implantation of any artificial corneal device, e.g., intracorneal stromal rings to correct refractive errors (4, 5), Boston keratoprosthesis (6–8), and osteo-odonto keratoprosthesis (OOKP) (9, 10) used to restore vision in patients with end-stage corneal blindness. Patients with endophthalmitis present with discharge, lid swelling, pain, reduced vision acuity, implant erosion, or exposure (11). Infected patients normally receive systemic or local antibiotic/antifungal treatment once their infection has been diagnosed, and implant removal is sometimes required. Implant-related infections are generally difficult to manage, result in an adverse effect on patient quality of life, require prolonged hospital admission, and culminate in a higher final cost to the patient and the health care provider (12, 13). Currently, there are limited strategies for preventing infections associated with surgical implants. Hence, clinically applicable and effective strategies are urgently needed to address this issue.

Both systemic and locally applied antibiotic agents have been used to prevent infections associated with surgical implants. Antimicrobial agents applied locally usually provide higher drug levels on the surface of devices and the immediate vicinity than does systemic administration (1). Various approaches to local prophylaxis have been tried to prevent bacterial colonization, including antimicrobial irrigation of the surgical field (such as sterilizing the ocular surface with povidone-iodine before ophthalmic surgery [14]), placement of antimicrobial carriers (e.g., intraoperative insertion of antibiotic-treated prosthetic devices in orthopedics [15]), dipping implants into antimicrobial solutions (e.g., immersion of a heart valve prosthesis into antibiotic solution before implantation [16]), and coating surgical implants with antimicrobials (17). Among these methods, coating implants with antimicrobials provides the unique advantage of potentially delivering the antimicrobial drug in a controllable manner via conditioned biodegradation of chemical bonds that cross-link the implant surface with the antimicrobial drugs. Clinical trials with the use of Silzone-coated St. Jude medical valves (18) or the use of silver-coated pins in orthopedics have proven that antimicrobial coatings are effective (19).

In previous studies, we showed that titanium (Ti) is a prospective biomaterial for synthetic osteo-odonto keratoprosthesis (OOKP) skirts, as it shows excellent biocompatibility (20) and Ti is stable in inhospitable environments often seen in ocular microbial infections (21, 22). We (23) and others (24, 25) previously showed the effectiveness of functionalized Ti with immobilized antimicrobial coatings *in vitro*. Compared with other antimicrobial agents, such as antibiotics, antimicrobial peptides (AMPs) have a broad spectrum of activity and possess a low propensity for developing pathogen resistance (26). Antimicrobial peptides can

Received 24 March 2014 Returned for modification 2 May 2014
Accepted 15 June 2014
Published ahead of print 23 June 2014
Address correspondence to Jodhbir S. Mehta, jodmehta@gmail.com.
Supplemental material for this article may be found at http://dx.doi.org/10.1128/AAC.02859-14.

doi:10.1128/AAC.02859-14
The authors have paid a fee to allow immediate free access to this article.

be effectively immobilized on Ti substrates by the use of a phosphate lipid spray or cross-linking agent, e.g., sinalization or polyethylene glycol (PEG) (27, 28). Despite several publications on the *in vitro* efficacy of AMPs (23–25), there are few studies demonstrating their efficacy *in vivo* (29). In the current study, we examined the effectiveness of a functionalized implant in a rabbit keratitis model for its potential application as an artificial cornea skirt to prevent perioperative corneal infection. The coating of a synthetic Ti OOKP with AMPs may improve the biocompatibility and bactericidal effect of an artificial corneal device for this group of patients with end-stage corneal diseases.

MATERIALS AND METHODS

MIC of soluble SESB2V. MICs were obtained in Mueller-Hinton broth (MHB) using the broth macrodilution method following CLSI guidelines (30). SESB2V peptide was dissolved in water to make 1,000-μg/ml stock solutions. Serial 2-fold dilutions of the peptide were prepared in cation-adjusted MHB in test tubes. The bacterial suspension was added in each tube to maintain a final concentration of approximately 5×10^5 CFU/ml. The tubes were then incubated at 35°C for 20 to 22 h. The bacterial growth was checked in all the test tubes and tabulated for each concentration as "growth" or "no growth." The MIC of the peptide was defined as the lowest concentration that prevented the visible growth of bacteria.

Preparation of substrates and SESB2V peptide coating. The SESB2V and truncated peptides were purchased from EZBiolab Inc. (Carmel, IN). The Ti substrate and AMP coating were prepared as previously described (23). Briefly, Ti substrates were cleaned ultrasonically for 10 min each in dichloromethane, acetone, and water and placed in HNO_3 (40%) for 40 min for surface passivation. Acid-treated titanium substrates were washed with ultrapure water before further treatment. For surface polydopamine (PDOP) coating, the titanium substrates were immersed in a dopamine hydrochloride solution (2 mg/ml) that was dissolved in Tris buffer (10 mmol, pH 8.5) for 12 h in darkness. The PDOP-coated substrates were then coated with the SESB2V solution (500 μg/ml) on both surfaces. After being briefly washed with phosphate-buffered saline (PBS), modified substrates were stored at 4°C prior to further analysis. Thin (0.005-mm-thickness) Ti films (Goodfellow, Cambridge, United Kingdom) were used for *in vitro* peptide stability testing and *in vivo* studies. For *in vitro* peptide stability testing, fluorescein isothiocyanate (FITC)-conjugated SESB2V peptide was immobilized onto the Ti surface. The functionalized substrate films were then soaked in PBS and kept in the dark. Fluorescence images were captured by a camera attached to a microscope (Axioplan 4.4; Carl Zeiss, Gottingen, Germany).

Bactericidal activities of SESB2V peptide. The bactericidal function of SESB2V was analyzed with a Live/Dead BacLight bacterial viability kit (Molecular Probes, Carlsbad, CA). *Staphylococcus aureus* (ATCC 29213) and *Pseudomonas aeruginosa* (ATCC 9027) were used for the bactericidal assays. Yeast extract-dextrose broth containing peptone (10 g/liter), beef extract (8 g/liter), sodium chloride (5 g/liter), glucose (5 g/liter), and yeast extract (3 g/liter) was used as the growth medium. The bacteria were incubated overnight at 37°C with agitation and then washed and resuspended in phosphate-buffered saline (PBS) at an optical density at 600 nm (OD_{600}) of 1.5. A bacterial suspension (500 μl) was then added to each substrate in a 24-well plate and incubated for 30 min at 37°C. The substrates ($n = 3$ for each) were then rinsed with PBS to remove nonadherent bacteria before analyzing with the protocol provided by the manufacturer. Images of live/dead bacteria were taken with a fluorescence microscope (Carl Zeiss), and images of six areas were randomly captured. The numbers of live/dead bacteria in each image were counted in three replicates.

Animal surgery. The animal protocol of the study adhered to the Statement for Use of Animals in Ophthalmic Vision and Research by the Association for Research in Vision and Ophthalmology. The protocol was approved by the Institutional Animal Care and Use Committee and Institutional Biosafety Committee at the Singapore Eye Research Institute.

Thirty-six New Zealand White rabbits, aged 1 to 2 months and weighing 2 to 2.5 kg, were used in the study. The animals were anesthetized using an intramuscular injection of ketamine hydrochloride (35 mg/kg of body weight; Parnell Laboratories, Alexandria, Australia) and xylazine hydrochloride (5 mg/kg; Troy Laboratories, Smithfield, Australia). The right eye of each rabbit was chosen for surgery. The contralateral eye of the implanted rabbit served as the control. Following anesthesia, a 7-mm-diameter and 75% deep corneal stromal pocket was created using a VisuMax femtosecond laser machine (Carl Zeiss Meditec, Jena, Germany). A 5-mm-wide circumferential incision was made by a guarded diamond knife (Storz; Bausch and Lomb). While forceps gently held the anterior flap in place, a Siebel spatula was inserted to separate the cornea along the laser-created pocket. A 4-mm-diameter implant film was then inserted into the pocket. Following insertion, the incision was then closed with interrupted 10/0 nylon sutures (see Fig. S1A to C in the supplemental material).

All the rabbits received topical medications immediately after implantation, including 0.3% tobramycin (Tobrex; Alcon Laboratory, Inc., Fort Worth, TX) and 1% prednisolone acetate (Pred Forte; Allergan, Irvine, CA). At 1 week postoperation, a 50-μl bacterial solution (2×10^4 CFU/ml) was inoculated into the corneal pocket above the titanium discs with a syringe attached to a 29-gauge needle (Fig. 1D). For rabbits with corneas with pristine Ti implants ($n = 21$), one group was sacrificed at day 2 after inoculation of *S. aureus* ($n = 9$) or *P. aeruginosa* ($n = 6$), and the other group ($n = 6$) received antibiotic eye drops immediately after *S. aureus* ($n = 3$) or *P. aeruginosa* ($n = 3$) inoculation. The antibiotics used were 0.3% gatifloxacin eye drops (Zymar) (one drop every 2 h) and an antibiotic solution (100 μl of 330 mg/ml cefazolin and 100 μl of 40 mg/ml gentamicin) injected subconjunctivally once a day. The group of rabbits that received the antibiotic solution ($n = 6$) were sacrificed after treatment with antibiotics continuously for 2 days. The rabbits with corneas with Ti-AMP implants ($n = 15$) were also divided into 2 groups. One group of rabbits was followed until day 2 after inoculation of the bacteria ($n = 6$ for *S. aureus* and $n = 3$ for *P. aeruginosa*), and another group of rabbits ($n = 3$ for *S. aureus* and $n = 3$ for *P. aeruginosa*) was followed until day 7 postinoculation. The study design is pictured in Fig. 1.

Slit lamp imaging and anterior segment optical coherence tomography. Slit lamp photographs and anterior segment optical coherence tomograms (AS-OCT) were taken on the days before and after Ti implantation, the day before bacterial inoculation, and days 1, 2, and 7 after bacterial inoculation. Slit lamp photographs were taken with a Zoom slit lamp NS-2D (Righton, Tokyo, Japan). Postinfection corneal slit lamp images were graded by a scoring method reported by Johnson et al. (31). Briefly, the infection grade (0 to 4) is based on the evaluation of the following infection symptoms: none to severe conjunctival infection, none to severe chemosis, none to severe iritis (cell and flare), none to severe fibrin formation, the area of hypopyon formation, the area of stromal infiltration (percentage of stroma with white cell infiltrate), and the area of stromal edema (percentage of stroma which is swollen). Corneal cross-sectional visualization was performed with a Visante AS-OCT (Carl Zeiss). Corneal thicknesses were measured using the software provided by the manufacturer.

Quantification of viable bacteria from infected rabbit corneas. At the determined time points, the infected eyes (both controls and treated) were enucleated from the rabbits and used for bacterial quantification. The corneas were dissected from the rest of the eye ball and individually homogenized in sterile phosphate-buffered saline (PBS) using plastic pestles followed by fine homogenization with bead beating using sterile glass beads (2 mm). The homogenate then underwent serial dilution plating using Trypticase soy agar (TSA) plates (Beckman, USA). The plates were incubated at 35°C for 48 h. The numbers of colonies were counted, and the results are expressed as the $\log_{10}$ number of CFU/cornea.

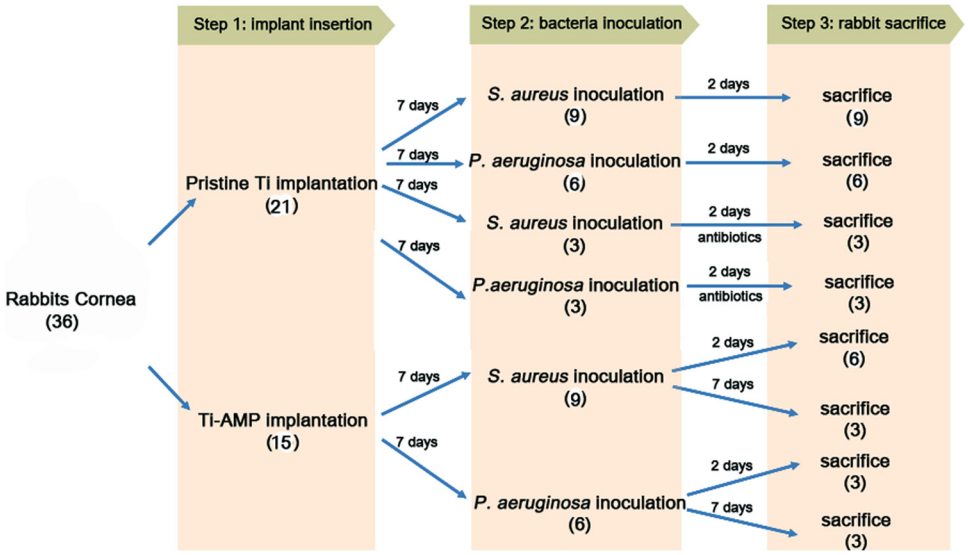

FIG 1 Design of the rabbit study.

Tissue fixation and sectioning. After euthanization, the rabbit corneas were removed and postfixed in 4% paraformaldehyde, followed by dehydration with a serial concentration of ethanol. After dehydration, tissue blocks were embedded into paraffin for hematoxylin-eosin (H&E) staining. For immunostaining, following fixation, tissues blocks were embedded in optimum cutting temperature (OCT) cryocompound (Leica Microsystems, Nussloch, Germany). Frozen tissue blocks were stored at −80°C until sectioning. Serial sagittal corneal 10-μm sections were cut using a cryostat (Microm HM550; Microm, Walldorf, Germany). Sections were placed on polylysine-coated glass slides and air dried for 15 min.

H&E and immunofluorescent staining. For H&E staining, tissue sections were immersed in hematoxylin (Sigma-Aldrich, Oakville, Canada) and eosin (Sigma) solutions for 10 to 20 s before cleaning with pure xylene. For immunostaining, tissue sections were postfixed with 4% paraformaldehyde for 15 min, washed with 1× PBS, and blocked with 10% normal goat serum in 1× PBS and 0.15% Triton X-100 for 1 h. The sections were incubated with either rat monoclonal antibody against CD11b (Abcam, San Francisco, CA) diluted 1:100, rat monoclonal antibody against F4/80 (Abcam) diluted 1:50, or mouse monoclonal antibody against MMP9 (Sigma) diluted 1:200 at 4°C overnight. After washing with 1× PBS, the sections were incubated with goat anti-mouse or goat anti-rat Alexa Fluor 488-conjugated secondary antibody (Invitrogen, Carlsbad, CA) at room temperature for 1 h. Slides were then mounted with UltraCruz mounting medium containing 4′,6-diamidino-2-phenylindole (DAPI) (Santa Cruz Biotechnology, Santa Cruz, CA). For negative controls, nonimmune serum was used in place of the specific primary antibody. Sections were observed and imaged with a fluorescence microscope (Carl Zeiss).

Statistical analysis. Data are presented as means ± the standard errors (SE). The *P* value was determined using one-way analysis of variance (ANOVA) with Microsoft Excel 2007 software (Microsoft, Redmond, WA). The Student *t* test was used for counting the live/dead bacterial ratios. Data were considered to be statistically significant when the *P* value was <0.05.

RESULTS

Previous studies have indicated that incubation of the full-length peptide with trypsin generates a number of proteolytically processed fragments and a partial loss of antimicrobial activities in the presence of tear fluid (32). Since the microenvironment in the stroma encompasses a number of proteases, we sought to investigate the efficacy of the full-length SESB2V peptide and its various sequentially truncated variants. First, we determined the MICs of full-length and truncated peptides against *S. aureus* and *P. aeruginosa* strains. As shown in Fig. 2A, the MICs of truncated peptides to *S. aureus*, except the shortest peptide, [(R)2*K*]2*K*K, varied from 3.125 μg/ml to 25 μg/ml. The MIC of the full-length peptide, [(RGRKVVRR)2*K*]2*K*K, was 6.125 μg/ml. For *P. aeruginosa* the MICs of the truncated peptides, except [(VVRR)2*K*]2*K*K and [(R)2*K*]2*K*K, varied from 6.25 μg/ml to 25 μg/ml. The MIC of the full-length peptide was 12.5 μg/ml. These results indicate that SESB2V peptide retained a high bactericidal effect on the *S. aureus* and *P. aeruginosa* strains even after truncation.

We then studied the *in vitro* bactericidal effect of the immobilized AMP with a Live/Dead bacterial imaging assay. Clusters of live bacteria (stained green) were seen on pristine Ti substrates (Fig. 2B), while on SESB2V-functionalized Ti substrates, most of the bacteria were dead (stained red). The quantitative live/dead ratio of bacteria was calculated to compare the antimicrobial properties of the pristine Ti and Ti-AMP substrates (Fig. 2B). The mean live/dead ratios of *S. aureus* and *P. aeruginosa* cells on pristine Ti substrates (15.8:1 for *S. aureus* and 1.66:1 for *P. aeruginosa*) were significantly higher than those on Ti-AMP substrates (2.5:1 for *S. aureus* [$P = 0.01$ compared to the Ti group] and 0.48:1 for *P. aeruginosa* [$P = 0.03$ compared to the Ti group]).

We also studied the stability of the AMP coating on Ti metal substrates *in vitro*. The fluorescence signal of the FITC-conjugated SESB2V peptide (SESB2V-FITC) lasted at least 60 days after covalent binding onto Ti substrates (Fig. 2C). Pristine Ti showed no fluorescence after laser excitation by the same microscope.

The bactericidal effects of AMP were tested in a rabbit keratitis model. No clinical signs of toxicity were observed in any rabbit eyes after Ti or Ti-AMP implantation. After the *S. aureus* bacterial injection, signs of inflammation and infection were visible clinically in the pristine Ti-implanted rabbits by day 1 postinoculation ($n = 9/9$), and there was worsening in seven of the nine eyes by day 2. Clinical symptoms included conjunctival chemosis, discharge,

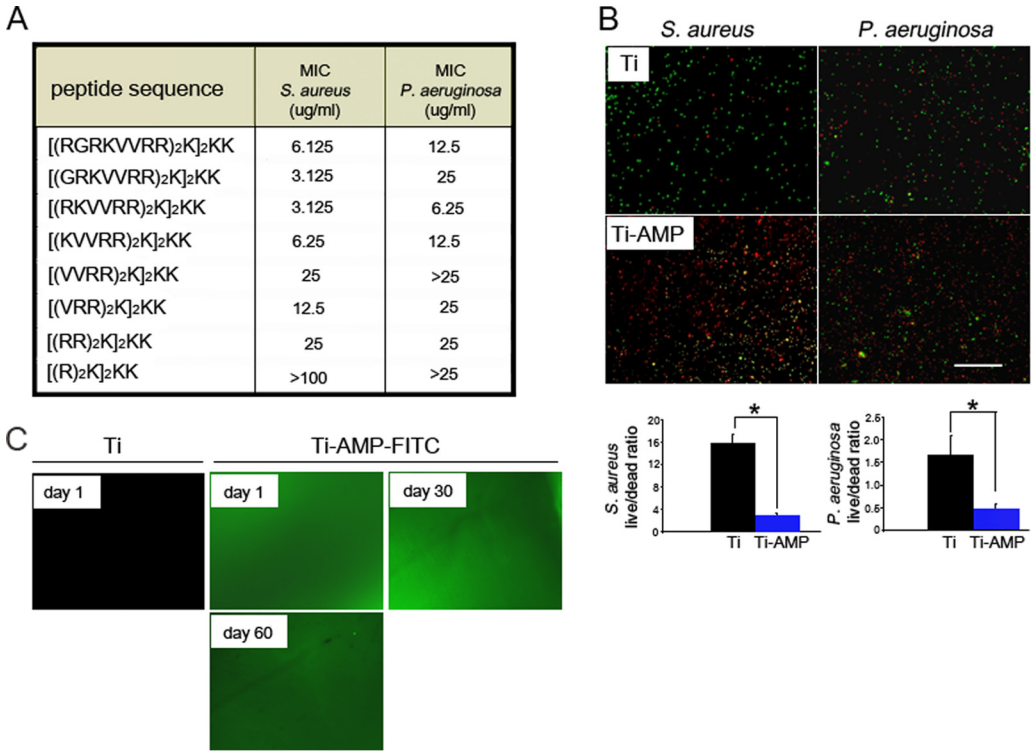

FIG 2 *In vitro* bactericidal effect and stability of SESB2V AMP. (A) MICs of the full-length and truncated SESB2V peptides. (B) Representative images from the Live/Dead bactericidal assay. Green, live bacteria; red, dead bacteria. The live/dead ratios were determined and graphed. *, $P < 0.05$ ($n = 6$, Student's *t* test). (C) Fluorescence images of Ti surface after immobilization with SESB2V-FITC peptide in phosphate-buffered saline.

hypopyon in the anterior chamber, severe corneal edema, and iritis. Most of the corneas ($n = 5/9$) melted due to severe edema, inflammatory cellular infiltration, and cell sloughing. However, for the corneas with Ti-AMP implants, most of the corneas ($n = 7/9$) developed no obvious signs of inflammation and remained clear after bacterial inoculation. Three eyes were followed up to 7 days. Two of the three eyes still had minimal signs of infection/inflammation up to day 7 postinoculation (Fig. 3A). For rabbits with the *P. aeruginosa* inoculation, signs of inflammation and infection occurred in corneas with both pristine Ti ($n = 6/6$) and AMP-coated Ti ($n = 4/6$) implants on day 1 postinoculation and worsened on day 2 postinoculation ($n = 6/6$ for pristine Ti group and $n = 4/6$ for Ti-AMP group). However, for corneas with Ti-AMP implants, the infection was localized to the central area of the cornea and was not as extensive compared with that in the pristine Ti implants. On day 7 postinoculation, there were still signs of localized inflammation and infection in the Ti-AMP group ($n = 2/3$) (see Fig. S2A in the supplemental material). Due to the severe melting of the corneas, the rabbits in the pristine Ti implantation group were sacrificed at day 2 postinoculation; hence, there were no data collected at day 7 from this group.

Table 1 summarizes the mean ocular infection score for each bacterial inoculum group obtained by slit lamp examination. In the pristine Ti implant group, all of the eyes ($n = 9$) developed signs of bacterial *S. aureus* infection within 48 h postinoculation, while in the Ti-AMP implant group, two out of nine eyes developed signs of infection. The mean (±SE) ocular inflammation score for the Ti group was 2.78 ± 0.36 on day 1 postinoculation and 3.56 ± 0.18 on day 2 postinoculation, while the mean ocular inflammation score for the Ti-AMP group was 0.22 ± 0.15 on day 1 postinoculation, 0.56 ± 0.38 on day 2 postinoculation ($P = 0.01$ between the Ti and Ti-AMP groups at both day 1 and day 2 time points), and 0.34 ± 0.31 on day 7 postinoculation. As for the *P. aeruginosa* inoculation group, all six eyes with Ti implants developed severe signs of infection, and four of the six eyes with Ti-AMP implants developed mild to moderate signs of infection. The mean ocular inflammation score for the Ti group was 3.17 ± 0.33 on day 1 postinoculation and 3.67 ± 0.22 on day 2 postinoculation, while the mean ocular inflammation score for the Ti-AMP group was 1 ± 0.39 on day 1 postinoculation, 1.67 ± 0.78 on day 2 postinoculation ($P = 0.01$ between the Ti and Ti-AMP groups at both day 1 and day 2 time points), and 1.33 ± 0.67 on day 7 postinoculation.

On AS-OCT examination, the Ti film appeared as a hyperreflective line on the scanned image, confirming the position of the implant (Fig. 3B). Within 48 h of inoculation with *S. aureus*, the mean corneal thickness anterior to pristine Ti implants increased to 757 ± 76.7 μm, while the mean corneal thickness anterior to Ti-AMP implants increased to 408 ± 37 μm ($P = 0.02$ between the Ti and Ti-AMP groups). At day 7 postinoculation, the mean corneal thickness was 360 ± 12.3 μm in the Ti-AMP group (Fig. 3C). Infection of the AMP-coated Ti corneas was worse after *P. aeruginosa* inoculation than that after *S. aureus* inoculation. Within 48 h of *P. aeruginosa* inoculation, the mean corneal thickness anterior to pristine Ti implants increased to 1,010.7 ± 225.4 μm, while the mean corneal thickness anterior to Ti-AMP implants increased to 460.3 ± 100.1 μm ($P = 0.01$ between the Ti and Ti-AMP groups). At day 7 postinoculation, the mean corneal

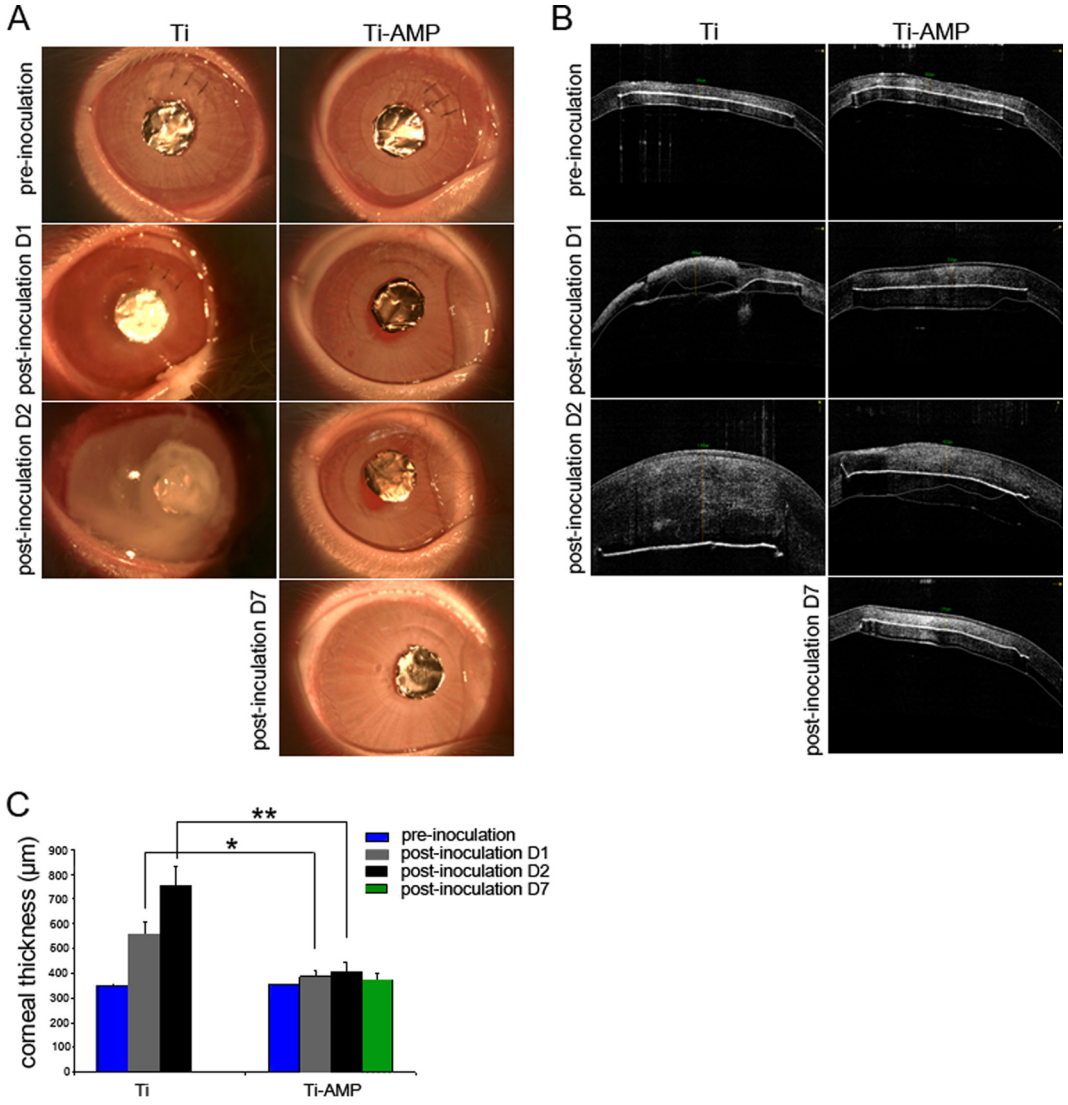

FIG 3 *In vivo* bactericidal effect of SESB2V AMP against *S. aureus*. (A) Slit lamp examination of the rabbit eyes before and after implantation and bacterial inoculation. (B) AS-OCT scanning of the rabbit eyes before and after implantation and bacterial inoculation. (C) Measurement of corneal thickness. Only corneal thickness anterior to the implant was measured at pre- and postinoculation day 1 and day 2. *, $P < 0.05$ (one-way ANOVA) between the pristine Ti and Ti-AMP groups at postinoculation day 1; **, $P < 0.05$ (one-way ANOVA) between the pristine Ti and Ti-AMP groups at postinoculation day 2.

thickness of the Ti-AMP group was 409.2 ± 31.4 μm (see Fig. S2C in the supplemental material).

We counted bacterial clones from the rabbits' corneal tissue to analyze the bacterial loads. By 48 h postinoculation, the number of *S. aureus* organisms increased from the initial inoculum of 1,000 CFU per cornea to approximately 1.3×10^7 CFU per cornea in the Ti group and increased to 6.6×10^3 CFU per cornea in the Ti-AMP group ($P = 0.01$ between the Ti and Ti-AMP groups). At day 7 postinoculation, there was no bacterial growth in the Ti-AMP group culture plates. Similarly, within 48 h of bacterial inoculation, the number of *P. aeruginosa* organisms increased from the initial inoculum of 1,000 CFU per cornea to approximately 1.9×10^6 CFU per cornea in the Ti group and 9.4×10^3 CFU per cornea in the Ti-AMP group ($P = 0.01$ between the Ti and Ti-AMP groups). At day 7 postinoculation, there was 1.74×10^2 CFU per cornea in the Ti-AMP group (Fig. 4).

Tissue sections were analyzed to further evaluate inflammatory responses following bacterial inoculation. At 48 h postinoculation, H&E staining of *S. aureus*-infected corneas with a pristine Ti implant revealed loss of corneal integrity as a result of melting of the epithelial layer in the central cornea (Fig. 5B). Blood vessels grew into the corneal stroma (Fig. 5C), and inflammatory cells infiltrated the central cornea surrounding the area of the implant pocket (Fig. 5C). However, *S. aureus*-infected corneas with a Ti-AMP implant revealed very mild cellular infiltration (Fig. 5E and F), and the keratocyte nuclei were aligned as they would be in a normal cornea (Fig. 5G).

In corneas with a pristine Ti implant, the inflammatory markers CD11b, F4/80, and MMP9 were all highly expressed in the anterior corneal stroma area, while there was reduced expression in the corneas of the Ti-AMP implant group (Fig. 6). For the *P. aeruginosa*-infected group, similar different patterns of inflamma-

TABLE 1 Scoring of corneal infection from slit lamp examinations

Bacterium	Rabbit no. (pristine Ti group)	Infection score on postinoculation day: 1	2	Rabbit no. (Ti-AMP group)	Infection score on postinoculation day: 1	2	7
S. aureus	I	2	3	I	0	0	0
	II	2	3	II	1	2	1
	III	1	3	III	0	0	0
	IV	4	4	IV	0	0	
	V	4	4	V	0	0	
	VI	3	4	VI	0	0	
	VII	4	4	VII	0	0	
	VIII	3	4	VIII	1	3	
	IX	2	3	IX	0	0	
Mean ± SE		2.78 ± 0.36	3.56 ± 0.18		0.22 ± 0.15	0.56 ± 0.38	0.34 ± 0.31
P. aeruginosa	I	2	3	I	0	0	0
	II	3	4	II	2	3	3
	III	3	4	III	2	3	2
	IV	3	3	IV	1	2	
	V	4	4	V	0	0	
	VI	4	4	VI	1	2	
Mean ± SE		3.17 ± 0.33	3.67 ± 0.22		1 ± 0.39	1.67 ± 0.78	1.33 ± 0.67

tory cell infiltration were observed in the corneas with a pristine Ti or AMP-coated Ti implant (see Fig. S3 and S4 in the supplemental material).

We compared the bactericidal effect of immobilized AMP with postinfective antibiotics. At day 1 of antibiotic treatment, all three rabbits still had severe clinical signs of *S. aureus* infection, with an average infection score of 3.67 ± 0.33. At day 2 of treatment, the signs improved with an average score of 2.67 ± 0.33 (Fig. 7A). In the corneas that received antibiotic treatment, the number of *S. aureus* organisms increased from the initial inoculum of 1,000 CFU to 8.3×10^4 CFU per cornea (Fig. 7B), which was significantly higher ($P = 0.02$) than that in the Ti-AMP group at postinoculation day 2 (6.6×10^3 CFU per cornea). For rabbits with *P. aeruginosa* inoculation and antibiotic treatment, the corneas developed mild clinical signs of keratitis, with an averaged infection score of 1.67 ± 0.33 at day 1, and there were no obvious clinical signs of corneal infection at day 2 of treatment (Fig. 7C). No *P. aeruginosa* organisms were cultivated from the corneal tissue (Fig. 7D).

DISCUSSION

An artificial corneal device bridges the nonsterile ocular surface with the sterile anterior chamber. There is a high risk of rapid invasion of bacterial pathogens into the corneal stroma where the artificial cornea device is situated. Our objective in this study was to develop a local administrative antimicrobial approach to inhibit the bacterial colonization on an implant placed into a cornea. AMP (SESB2V) was immobilized onto the surface of Ti via a

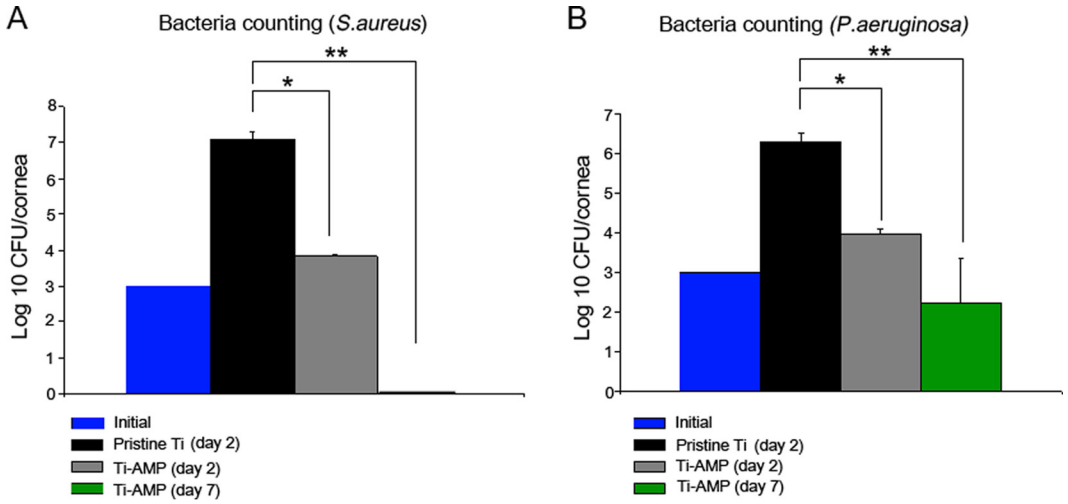

FIG 4 Bacteria counts of *S. aureus* and *P. aeruginosa* cells. Results are presented as $\log_{10}$ CFU/cornea ± standard error of the mean (SEM). * and **, $P < 0.05$ ($n = 3$ in each group; one-way ANOVA).

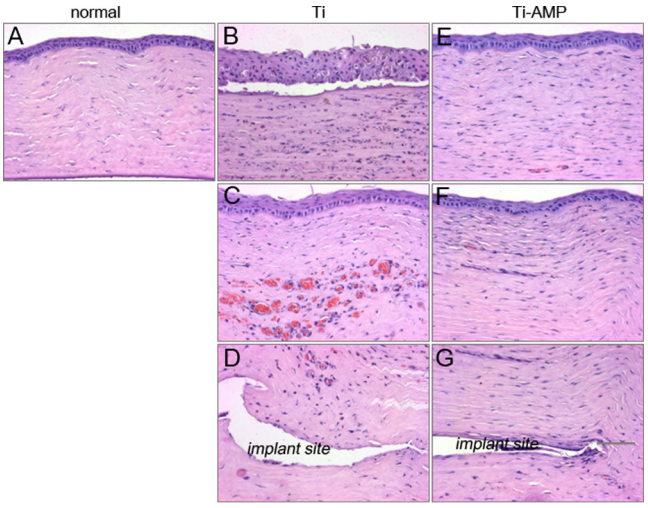

FIG 5 Hematoxylin-eosin (H&E) pictures of rabbit corneas after inoculation with *S. aureus*. (A) Normal rabbit cornea. (B to D) Rabbit cornea with pristine Ti implantation and bacterial infection: corneal epithelium (B), central corneal stroma (C), and corneal stroma surrounding the implant pocket (D). (E to G) Rabbit cornea with Ti-AMP implantation and bacterial infection: corneal epithelium (E), central corneal stroma (F), and corneal stroma surrounding the implant pocket (G).

cross-linker, polydopamine (33, 34). To mimic keratoprosthesis surgery, Ti films were then inserted into rabbit corneal stromal pockets. Ti implants whose surfaces were functionalized with AMP efficiently inhibited corneal bacterial infections with minimal adjacent tissue damage. Immobilized AMP proved to be more efficient *in vivo* against *S. aureus* than against *P. aeruginosa*. We also demonstrated that the Ti-AMP implants showed superior bactericidal activity against *S. aureus* compared to the use of post-inoculation topical antibiotics.

Current strategies for combating implant-associated ocular infections include the continuous use of topical antibiotics (1). However, a serious concern regarding the continuous use of conventional antibiotics is the potential development of antibiotic-resistant pathogens such as methicillin-resistant *Staphylococcus aureus* (MRSA) (35–37) and fungi (7). Antibiotic-resistant infections can lead to devastating effects and uncontrolled bacterial infection. Therefore, AMPs that have a wide spectrum of bactericidal activity and that are less likely to develop bacterial resistance (26, 37) are an ideal substitute. There have been few studies on the *in vivo* efficacy of covalently bound AMPs. Gao et al. demonstrated the efficacy of AMP-coated Ti wire used in orthopedic surgery in a dorsal skin pocket model of wound infection (29).

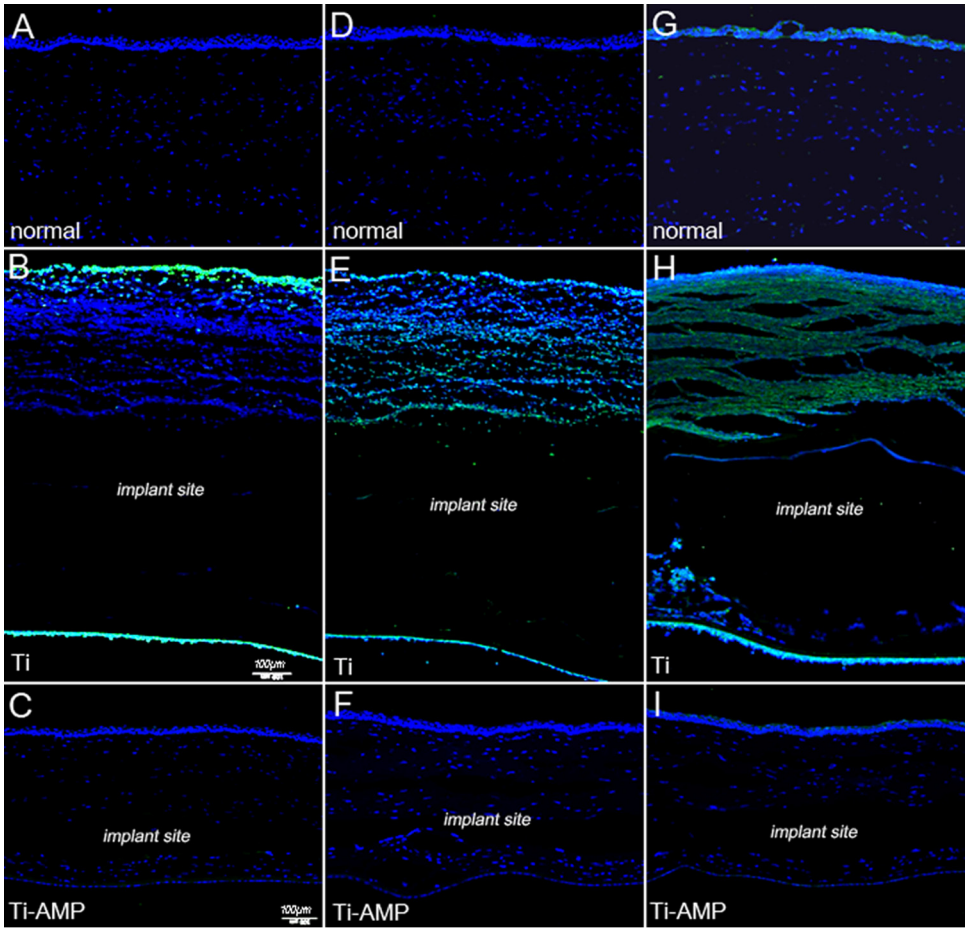

FIG 6 Immunostaining pictures of rabbit corneas after infection with *S. aureus*. Green, inflammatory cell markers; blue, DAPI cell nucleus counterstaining. (A to C) CD11b staining: normal rabbit cornea (A), cornea with pristine Ti implant (B), and cornea with Ti-AMP implant (C). (D to F) F4/80 staining: normal rabbit cornea (D), cornea with pristine Ti implant (E), and cornea with Ti-AMP implant (F). (G to I) MMP9 staining: normal rabbit cornea (G), cornea with pristine Ti implant (H), and cornea with Ti-AMP implant (I).

A

Rabbit Number (antibiotics)	Infection Score (D1)	Infection Score (D2)
I	4	3
II	3	2
III	4	3
mean±SE	3.67±0.33	2.67±0.33

B

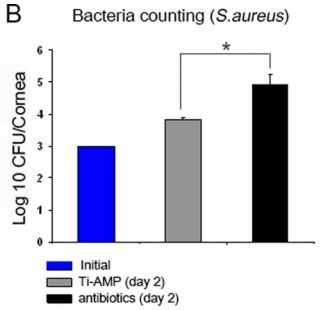

C

Rabbit Number (antibiotics)	Infection Score (D1)	Infection Score (D2)
I	2	0
II	2	0
III	1	0
mean±SE	1.67±0.33	0±0

D

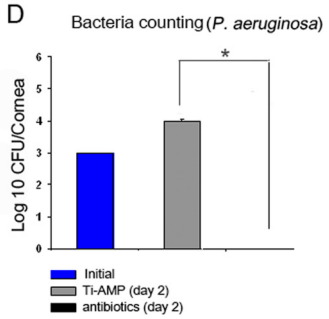

FIG 7 Antibiotic treatment of rabbit corneas after inoculation with *S. aureus* and *P. aeruginosa*. (A and C) Scoring of slit lamp examinations after inoculation of *S. aureus* (A) and *P. aeruginosa* (C). (B and D) Bacterium counting of corneal tissue after inoculation of *S. aureus* (B) and *P. aeruginosa* (D). *, $P < 0.05$ (one-way ANOVA).

Here, we report the successful surface functionalization of a metallic implant with immobilized AMP in an infectious keratitis model. In contrast to other studies, our model mimics precisely the clinical *in situ* placement of synthetic artificial cornea devices (29). We previously proved that SESB2V has a wide spectrum of bactericidal activity against Gram-positive and Gram-negative bacteria (23). We also determined the MIC of SESB2V against MRSA (DM21455) to be 6.25 μg/ml. In this study, we showed a low MIC (3.125 to 25 μg/ml) of soluble SESB2V and its truncated peptides against Gram-positive *S. aureus* and Gram-negative *P. aeruginosa* bacterial strains. These results indicate that fragmented SESB2V peptide still maintained a bactericidal effect, which is important clinically following protease digestion *in vivo*. These properties make SESB2V peptide a promising candidate for ocular therapeutic use. After immobilization onto Ti substrates, SESB2V peptide retained its bactericidal activities against *S. aureus* and *P. aeruginosa*, with a coating concentration of 500 μg/ml, which is about 80 times higher than the MICs of soluble SESB2V. We used this concentration, since the covalent binding of the AMP to the substrate surface is likely to alter the MIC. Previous studies have shown higher MICs of immobilized AMPs compared to those of soluble peptides (39–41). The difference in the live/dead ratio between *S. aureus* and *P. aeruginosa* cells on a pristine Ti surface is possibly because *P. aeruginosa* contains much higher levels of dead/weakened bacteria. Another possibility is that pristine Ti itself has a different bactericidal effect on different bacterial strains. However, these results are still valid, since we compared the live/dead ratio of bacteria before and after AMP immobilization.

Titanium films with immobilized SESB2V peptide were placed into the rabbits' corneal stroma, and there were no clinical signs of corneal inflammation within 1 week after implantation compared to those with a pristine Ti implant. AMPs have been shown to have immunomodulatory activities that include angiogenesis, modulation of cytokine activity, and reduction of lipopolysaccharide (LPS)-mediated proinflammatory responses (42, 43). The cytotoxicity associated with AMPs is usually related to the high concentrations used to compensate for their relatively short half-lives due to rapid tissue protease digestion (44). Covalent immobilization of SESB2V may decrease the long-term cytotoxicity to corneal tissue, since covalent binding would prolong the life span and function of the peptides and reduce the necessity for using high concentrations of AMP (44, 45). We observed that SESB2V was stable in a humidified environment for at least 2 months after immobilization onto a Ti surface. Additionally, the bactericidal effect of functionalized Ti discs may be achieved even after 2 weeks of implantation (1 week after bacterial inoculation). The results indicate that AMP activity was still present, even though these peptides may face the risk of degradation by tissue protease. The degraded product of SESB2V may still possess the bactericidal effect *in vivo*, as evidenced by the low MIC of the truncated SESB2V peptides. However, we observed a difference in the bactericidal efficacy of the AMP-coated implants against both *S. aureus* and *P. aeruginosa* at day 7 postinoculation (2 weeks after implantation). This was possibly due to the biodegradation or dysfunction of SESB2V peptide in the corneal stroma. Our results are encouraging for the early postoperative period, but bacterial endophthalmitis may occur months or years after the placement of a device (4–6). Hence, future work should examine the role of AMPs combined with a controlled drug delivery system, e.g., nanoparticles or biodegradable films.

The clinical score of corneal inflammation on slit lamp images and the quantitative analysis of corneal thickness on AS-OCT images, as well as the histological studies, demonstrated that immobilized SESB2V significantly reduced corneal inflammation and stromal swelling caused by either *S. aureus* or *P. aeruginosa* pathogens. Moreover, immobilized SESB2V was more effective in preventing postimplantation infection caused by *S. aureus* than that caused by *P. aeruginosa*. After the inoculation of *S. aureus* in the AMP-coated implants, the clinical analysis and histological images revealed less obvious signs of infection/inflammation than in those inoculated with *P. aeruginosa*. This was possibly because *P. aeruginosa* was less sensitive to the bactericidal activities of SESB2V peptide than the same inoculum of *S. aureus*. Additionally, we observed that the inoculation of *S. aureus* or *P. aeruginosa* caused the infiltration of different types of inflammatory cells in the absence of AMP. For example, an inoculation of *S. aureus* caused the infiltration of more F4/80-positive cells near the implant site, while an inoculation of *P. aeruginosa* caused the infiltration of more CD11b-positive cells. Hence, we cannot exclude the possibility that the difference in the bactericidal effects was due to the difference in the virulence of the pathogens (46, 47). The rabbits developed a more severe keratitis after *P. aeruginosa* inoculation than after *S. aureus* inoculation, even without the presence of AMP. However, the superior efficacy against *S. aureus* is clinically advantageous, since *S. aureus* is the leading cause of endophthalmitis and bacterial keratitis after ocular implantation (7).

Following the clinical diagnosis of an ocular implant infection, the initial treatment will involve the use of intensive topical antibiotics. Hence, we compared the effect of intensive topical antibiotic therapy in a clinical situation similar to that of the immobi-

lized SESB2V treatment used in this study. Compared with topical antibiotics, there was a significantly lower clinical inflammation score and fewer bacterial clones with the AMP coating following *S. aureus* inoculation. However, the topical antibiotics were superior to SESB2V peptide in treating infections caused by *P. aeruginosa*, as the inflammatory symptoms resolved and there was no growth of bacterial clones after treatment by the current choice of antibiotics (Fig. 7C and D). In clinical reality, the topical therapy would be used as an adjunct to the AMP coating; hence, localized control of the infection by the AMP coating, as indicated by our results, may prevent further spread of the infection into fulminant endophthalmitis.

Infections associated with the implantation of biomaterials remain one of the major barriers to the use of medical devices in patients. We have successfully immobilized a novel AMP to deliver a bactericidal effect *in vivo*. Hence, our study demonstrates the efficacy of a local antimicrobial prophylactic measure in preventing implant-associated corneal infections in an infectious keratitis model.

ACKNOWLEDGMENTS

We thank Mageswari D/O Muthusamy for assistance with animal techniques.

This work was supported by Singhealth Research Foundation (grant SHF/FG488S/2010).

REFERENCES

1. **Darouiche RO.** 2004. Treatment of infections associated with surgical implants. N. Engl. J. Med. **350:**1422–1429. http://dx.doi.org/10.1056/NEJMra035415.
2. **Baker AS, Schein OD.** 1989. Ocular infections, p 75–92. *In* Bisno L, Waldvogel FA (ed), Infections associated with indwelling medical devices. ASM Press, Washington, DC.
3. **Behlau I, Gilmore MS.** 2008. Microbial biofilms in ophthalmology and infectious diseases. Arch. Ophthalmol. **126:**1572–1581. http://dx.doi.org/10.1001/archopht.126.11.1572.
4. **Bourcier T, Borderie V, Laroche L.** 2003. Late bacterial keratitis after implantation of intrastromal corneal ring segments. J. Cataract Refract. Surg. **29:**407–409. http://dx.doi.org/10.1016/S0886-3350(02)01484-0.
5. **Shehadeh-Masha'our R, Modi N, Barbara A, Garzozi HJ.** 2004. Keratitis after implantation of intrastromal corneal ring segments. J. Cataract Refract. Surg. **30:**1802–1804. http://dx.doi.org/10.1016/j.jcrs.2004.01.034.
6. **Chan CC, Holland EJ.** 2012. Infectious keratitis after Boston type 1 keratoprosthesis implantation. Cornea **31:**1128–1134. http://dx.doi.org/10.1097/ICO.0b013e318245c02a.
7. **Robert MC, Moussally K, Harissi-Dagher M.** 2012. Review of endophthalmitis following Boston keratoprosthesis type 1. Br. J. Ophthalmol. **96:**776–780. http://dx.doi.org/10.1136/bjophthalmol-2011-301263.
8. **Nouri M, Terada H, Alfonso EC, Foster CS, Durand ML, Dohlman CH.** 2001. Endophthalmitis after keratoprosthesis: incidence, bacterial causes, and risk factors. Arch. Ophthalmol. **119:**484–489. http://dx.doi.org/10.1001/archopht.119.4.484.
9. **Hughes EH, Mokete B, Ainsworth G, Casswell AG, Eckstein MB, Zambarakji HJ, Gregor Z, Rosen PH, Herold J, Okera S, Liu CS.** 2008. Vitreoretinal complications of osteoodontokeratoprosthesis surgery. Retina **28:**1138–1145. http://dx.doi.org/10.1097/IAE.0b013e318174e10e.
10. **Tan A, Tan DT, Tan XW, Mehta JS.** 2012. Osteo-odonto keratoprosthesis: systematic review of surgical outcomes and complication rates. Ocul. Surf. **10:**15–25. http://dx.doi.org/10.1016/j.jtos.2012.01.003.
11. **Endophthalmitis Vitrectomy Study Group.** 1995. Results of the Endophthalmitis Vitrectomy Study, a randomized trial of immediate vitrectomy and of intravenous antibiotics for the treatment of postoperative bacterial endophthalmitis. Arch. Ophthalmol. **113:**1479–1496. http://dx.doi.org/10.1001/archopht.1995.01100120009001.
12. **Boxma H, Broekhuizen T, Patka P, Oosting H.** 1996. Randomised controlled trial of single dose antibiotic prophylaxis in surgical treatment of closed fractures: the Dutch Trauma Trial. Lancet **347:**1133–1137. http://dx.doi.org/10.1016/S0140-6736(96)90606-6.
13. **Whitehouse JD, Friedman ND, Kirkland KB, Richardson WJ, Sexton DJ.** 2002. The impact of surgical-site infections following orthopedic surgery at a community hospital and a university hospital: adverse quality of life, excess length of stay, and extra cost. Infect. Control Hosp. Epidemiol. **23:**183–189. http://dx.doi.org/10.1086/502033.
14. **Apt L, Isenberg S, Yoshimori R, Paez HJ.** 1984. Chemical preparation of the eye in ophthalmic surgery: III. Effect of povidone-iodine on the conjunctiva. Arch. Ophthalmol. **102:**728–729. http://dx.doi.org/10.1001/archopht.1984.01040030584025.
15. **Musella M, Guido A, Musella S.** 2001. Collagen tampons as aminoglycoside carriers to reduce postoperative infection rate in prosthetic repair of groin hernias. Eur. J. Surg. **167:**130–132. http://dx.doi.org/10.1080/110241501750070592.
16. **Actis Dato A, Jr, Chiusolo C, Cicchitti GC, Actis Dato GM, Porro MC, Bello A.** 1992. Antibiotic pretreatment of heart valve prostheses. Minerva Cardioangiol. **40:**225–229.
17. **Darouiche RO.** 2003. Antimicrobial approaches for preventing infections associated with surgical implants. Clin. Infect. Dis. **36:**1284–1289. http://dx.doi.org/10.1086/374842.
18. **Schaff H, Carrel T, Steckelberg JM, Grunkemeier GL.** 1999. Artificial Valve Endocarditis Reduction Trial (AVERT): protocol of a multicenter randomized trial. J. Heart Valve Dis. **8:**131–139.
19. **Masse A, Bruno A, Bosetti M, Biasibetti A, Cannas M, Gallinaro P.** 2000. Prevention of pin track infection in external fixation with silver coated pins: clinical and microbiological results. J. Biomed. Mater. Res. **53:**600–604. http://dx.doi.org/10.1002/1097-4636(200009)53:5<600::AID-JBM21>3.0.CO;2-D.
20. **Tan XW, Perera AP, Tan A, Tan D, Khor KA, Beuerman RW, Mehta JS.** 2011. Comparison of candidate materials for a synthetic osteo-odonto keratoprosthesis device. Invest. Ophthalmol. Vis. Sci. **52:**21–29. http://dx.doi.org/10.1167/iovs.10-6186.
21. **Pullamsetti SS, Savai R, Janssen W, Dahal BK, Seeger W, Grimminger F, Ghofrani HA, Weissmann N, Schermuly RT.** 2011. Inflammation, immunological reaction and role of infection in pulmonary hypertension. Clin. Microbiol. Infect. **17:**7–14. http://dx.doi.org/10.1111/j.1469-0691.2010.03285.x.
22. **Punnia-Moorthy A.** 1987. Evaluation of pH changes in inflammation of the subcutaneous air pouch lining in the rat, induced by carrageenan, dextran and *Staphylococcus aureus*. J. Oral Pathol. **16:**36–44. http://dx.doi.org/10.1111/j.1600-0714.1987.tb00674.x.
23. **Tan XW, Lakshminarayanan R, Liu SP, Goh E, Tan D, Beuerman RW, Mehta JS.** 2012. Dual functionalization of titanium with vascular endothelial growth factor and beta-defensin analog for potential application in keratoprosthesis. J. Biomed. Mater. Res. B Appl. Biomater. **100:**2090–2100. http://dx.doi.org/10.1002/jbm.b.32774.
24. **Behlau I, Mukherjee K, Todani A, Tisdale AS, Cade F, Wang L, Leonard EM, Zakka FR, Gilmore MS, Jakobiec FA, Dohlman CH, Klibanov AM.** 2011. Biocompatibility and biofilm inhibition of *N,N*-hexyl,methyl-polyethylenimine bonded to Boston keratoprosthesis materials. Biomaterials **32:**8783–8796. http://dx.doi.org/10.1016/j.biomaterials.2011.08.010.
25. **Kazemzadeh-Narbat M, Kindrachuk J, Duan K, Jenssen H, Hancock RE, Wang R.** 2010. Antimicrobial peptides on calcium phosphate-coated titanium for the prevention of implant-associated infections. Biomaterials **31:**9519–9526. http://dx.doi.org/10.1016/j.biomaterials.2010.08.035.
26. **Seo MD, Won HS, Kim JH, Mishig-Ochir T, Lee BJ.** 2012. Antimicrobial peptides for therapeutic applications: a review. Molecules **17:**12276–12286. http://dx.doi.org/10.3390/molecules171012276.
27. **Kazemzadeh-Narbat M, Lai BF, Ding C, Kizhakkedathu JN, Hancock RE, Wang R.** 2013. Multilayered coating on titanium for controlled release of antimicrobial peptides for the prevention of implant-associated infections. Biomaterials **34:**5969–5977. http://dx.doi.org/10.1016/j.biomaterials.2013.04.036.
28. **Gabriel M, Nazmi K, Veerman EC, Nieuw Amerongen AV, Zentner A.** 2006. Preparation of LL-37-grafted titanium surfaces with bactericidal activity. Bioconjug. Chem. **17:**548–550. http://dx.doi.org/10.1021/bc050091v.
29. **Gao G, Lange D, Hilpert K, Kindrachuk J, Zou Y, Cheng JT, Kazemzadeh-Narbat M, Yu K, Wang R, Straus SK, Brooks DE, Chew BH, Hancock RE, Kizhakkedathu JN.** 2011. The biocompatibility and biofilm resistance of implant coatings based on hydrophilic polymer brushes conjugated with antimicrobial peptides. Biomaterials **32:**3899–3909. http://dx.doi.org/10.1016/j.biomaterials.2011.02.013.

30. **Clinical and Laboratory Standards Institute.** 2009. Methods for dilution antimicrobial susceptibility tests for bacteria that grow aerobically; approved standard, 8th ed, M07-A8. Clinical and Laboratory Standards Institute, Wayne, PA.
31. **Johnson MK, Hobden JA, Hagenah M, O'Callaghan RJ, Hill JM, Chen S.** 1990. The role of pneumolysin in ocular infections with *Streptococcus pneumoniae*. Curr. Eye Res. **9:**1107–1114. http://dx.doi.org/10.3109/02713689008997584.
32. **Lakshminarayanan R, Liu S, Li J, Nandhakumar M, Aung TT, Goh E, Chang JY, Saraswathi P, Tang C, Safie SR, Lin LY, Riezman H, Lei Z, Verma CS, Beuerman RW.** 2014. Synthetic multivalent antifungal peptides effective against fungi. PLoS One **9:**e87730. http://dx.doi.org/10.1371/journal.pone.0087730.
33. **Lee H, Dellatore SM, Miller WM, Messersmith PB.** 2007. Mussel-inspired surface chemistry for multifunctional coatings. Science **318:**426–430. http://dx.doi.org/10.1126/science.1147241.
34. **Xie J, Michael PL, Zhong S, Ma B, MacEwan MR, Lim CT.** 2012. Mussel inspired protein-mediated surface modification to electrospun fibers and their potential biomedical applications. J. Biomed. Mater. Res. A **100:**929–938. http://dx.doi.org/10.1002/jbm.a.34030.
35. **Campoccia D, Montanaro L, Arciola CR.** 2006. The significance of infection related to orthopedic devices and issues of antibiotic resistance. Biomaterials **27:**2331–2339. http://dx.doi.org/10.1016/j.biomaterials.2005.11.044.
36. **Campoccia D, Montanaro L, Speziale P, Arciola CR.** 2010. Antibiotic-loaded biomaterials and the risks for the spread of antibiotic resistance following their prophylactic and therapeutic clinical use. Biomaterials **31:**6363–6377. http://dx.doi.org/10.1016/j.biomaterials.2010.05.005.
37. **Trampuz A, Zimmerli W.** 2006. Antimicrobial agents in orthopaedic surgery: prophylaxis and treatment. Drugs **66:**1089–1105. http://dx.doi.org/10.2165/00003495-200666080-00005.
38. **Park SC, Park YK, Hahm KS.** 2011. The role of antimicrobial peptides in preventing multidrug-resistant bacterial infections and biofilm formation. Int. J. Mol. Sci. **12:**5971–5992. http://dx.doi.org/10.3390/ijms12095971.
39. **Bagheri M, Beyermann M, Dathe M.** 2009. Immobilization reduces the activity of surface-bound cationic antimicrobial peptides with no influence upon the activity spectrum. Antimicrob. Agents Chemother. **53:**1132–1141. http://dx.doi.org/10.1128/AAC.01254-08.
40. **Cho WM, Joshi BP, Cho H, Lee KH.** 2007. Design and synthesis of novel antibacterial peptide-resin conjugates. Bioorg. Med. Chem. Lett. **17:**5772–5776. http://dx.doi.org/10.1016/j.bmcl.2007.08.056.
41. **Haynie SL, Crum GA, Doele BA.** 1995. Antimicrobial activities of amphiphilic peptides covalently bonded to a water-insoluble resin. Antimicrob. Agents Chemother. **39:**301–307. http://dx.doi.org/10.1128/AAC.39.2.301.
42. **Hale JD, Hancock RE.** 2007. Alternative mechanisms of action of cationic antimicrobial peptides on bacteria. Expert Rev. Anti Infect. Ther. **5:**951–959. http://dx.doi.org/10.1586/14787210.5.6.951.
43. **Jenssen H, Hancock RE.** 2010. Therapeutic potential of HDPs as immunomodulatory agents. Methods Mol. Biol. **618:**329–347. http://dx.doi.org/10.1007/978-1-60761-594-1_20.
44. **Chen R, Cole N, Willcox MD, Park J, Rasul R, Carter E, Kumar N.** 2009. Synthesis, characterization and *in vitro* activity of a surface-attached antimicrobial cationic peptide. Biofouling **25:**517–524. http://dx.doi.org/10.1080/08927010902954207.
45. **Costa F, Carvalho IF, Montelaro RC, Gomes P, Martins MC.** 2011. Covalent immobilization of antimicrobial peptides (AMPs) onto biomaterial surfaces. Acta Biomater. **7:**1431–1440. http://dx.doi.org/10.1016/j.actbio.2010.11.005.
46. **Karthikeyan RS, Priya JL, Leal SM, Jr, Toska J, Rietsch A, Prajna V, Pearlman E, Lalitha P.** 2013. Host response and bacterial virulence factor expression in *Pseudomonas aeruginosa* and *Streptococcus pneumoniae* corneal ulcers. PLoS One **8:**e64867. http://dx.doi.org/10.1371/journal.pone.0064867.
47. **Dajcs JJ, Thibodeaux BA, Girgis DO, O'Callaghan RJ.** 2002. Corneal virulence of *Staphylococcus aureus* in an experimental model of keratitis. DNA Cell Biol. **21:**375–382. http://dx.doi.org/10.1089/10445490260099656.